JEE Journal of Ecological Engineering

Journal of Ecological Engineering 2024, 25(7), 201–211
https://doi.org/10.12911/22998993/188274
ISSN 2299–8993, License CC-BY 4.0

Received: 2024.04.25
Accepted: 2024.05.16
Published: 2024.06.01

Thermal, Energy and Exergy Analysis of Thermoelectric Generator System for Waste Heat Recovery Applications

Ionescu Viorel[1*]

[1] Department or Physics and Electronics, Ovidius University of Constanta, Mamaia Bd. no. 124, 900527, Constanta, Romania

* Corresponding author's e-mail: ionescu.vio@gmail.com

ABSTRACT

The efficient recovery of the waste heat from the industrial sector can represent an essential step in global energy saving, with the proper usage of other on-grid power resources available for specific high-energy consumers. A simple, low–cost energy conversion system was tested here to recover a part of the waste heat dissipated by a gasoline engine's exhaust pipe under the car's stationary testing mode at temperatures around 80–100 °C. The main components of this system were a copper–made thermal collector, a commercial thermoelectric energy generator (TEG) module TEC1 – 12706 and a pin-fin heat sink under natural air convection cooling. Under the open-circuit test, heat transfer rates between 4.54 W and 5.56 W were evacuated by the heat sink. A DC electronic load R_L was connected at the TEG outputs, and voltage values between 0.566 V and 1.242 V were recorded for output power values between 0.03 W and 0.16 W when R_L was modified from 1 Ω to 10 Ω.

Keywords: heat rate, thermal resistance, output power, conversion efficiency.

INTRODUCTION

Generally, it is estimated that only about 20% of the current global energy is converted to useful work or new products, the rest of 80% being discharged into the environment as waste heat [1]. A temperature-based classification of waste energy resources was reported in the literature in the form of three main categories: low-grade (< 230 °C), medium-grade (650–230 °C) and high-grade (> 650 °C) waste [2]. As a result of the superior energy content, high-grade and medium-grade waste can be recovered in high amounts and reintroduced into the energy consumption cycle using technologies such as steam turbines and Rankine cycles [3]. The highest amount of environmentally dissipated heat, generated on a large scale within the usual industrial processes, is the low-grade waste heat. Due to the reduced temperature level, this type of waste is difficult to recover, and the cost–effective systems for efficient waste heat conversion to electrical power are still under development. Enhancing the heat transfer capacity from the waste heat source to the energy conversion device becomes fundamental for minimizing irreversible loss along this low-energy heat recovery process. For this reason, thermoelectric generator (TEG) – based heat recovery technology has attracted interest for its successful use in the heat recovery processes at temperatures under 200 °C [4]. Pipeline walls from the petrochemical industry generate a large amount of waste heat, but only at low temperatures, usually between 120–160 °C. So, improving the heat transfer capacity at the cold plate of TEG is crucial [6], and a suitable cooling method must be selected for the proper thermal design of the TEG – based energy conversion systems. The heat sinks can successfully assure heat transfer enhancement.

Passive cooling with natural air convection inside the heat sinks represents the first choice as the cooling method for the TEG – based energy conversion systems. In this case, no supplementary power consumption is required, negatively affecting the net output power. Still, passive cooling will introduce high thermal resistance values,

reducing TEG's energy conversion efficiency [7]. The air forced convection cooling with a fan was able to generate a constant decrease of temperature profile over the testing time [8]. The water cooling method will maintain a low and stable heat sink temperature, improving the thermoelectric energy conversion [9, 10]. Md. Asaduzzaman et al. [11] reported that a TEG system with a water-circulating bath comprising two commercial bismuth telluride (Bi_2Te_3) TEG modules placed on the exhaust gas pipe of an automotive engine generated about 0.8 W net output power at an exhaust temperature of 155 °C. Mohiuddin et al. [12] performed numerical simulations and experiments for a TEG energy conversion system with different types of heat sinks under natural air convection cooling. Their results showed that the rectangular fins had a better cooling performance than the circular tube fins placed on the heat sink structure. Another similar study developed by Boccardi et al. [13] showed that the heat sink with rectangular pin-fins improved by about 18% the maximum power output of the system at a TEG hot temperature of 100 °C, compared with the cylindrical pin shape heat sink. In this paper, we investigated the variation of the temperature gradient between the cold and hot plates of a commercial TEG module cooled by rectangular pin-fin heat sink under natural air convection and heated by an exhaust pipe at temperatures up to 110 °C.

THERMAL ANALYSIS OF THE SYSTEM

An image of the rectangular pin-fin heat sink used in the present energy conversion system, with details of geometrical parameters, is presented in Fig. 1. This heat sink, model ICK PEN 45 from Fisher Elektronik GmbH (Germany), was designed for Intel Pentium/MMX/AMD K6 microprocessors cooling.

The properties of the heat sink parameters considered here for thermal calculations are presented in Table 1. A simplified thermal resistance model of the energy conversion system is presented in Fig. 2, considering the copper–made thermal collectors placed between the TEG module and exhaust pipe as the heat source.

The total thermal resistance of the system part comprising the TEG module, thermal interface layers and the heat sink is calculated based on the relation:

Table 1. Heat sink parameters involved in the analysis

Symbol	Name	Value (mm)
L	Length of the sink base	50
H	Fin height	45
t	Sink base thickness	3.5
l	pin length	3.62
b	pin width	1.81

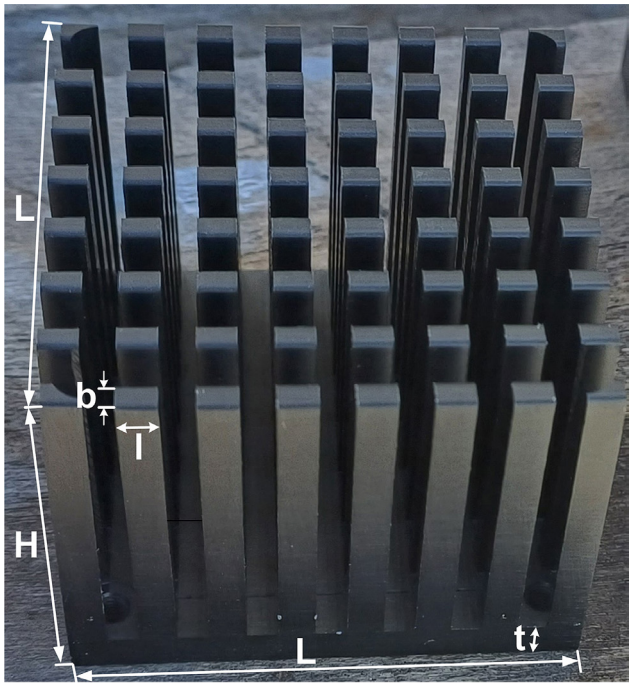

Figure 1. Picture of the pin-fin heat sink, with indications of the basic geometrical parameters

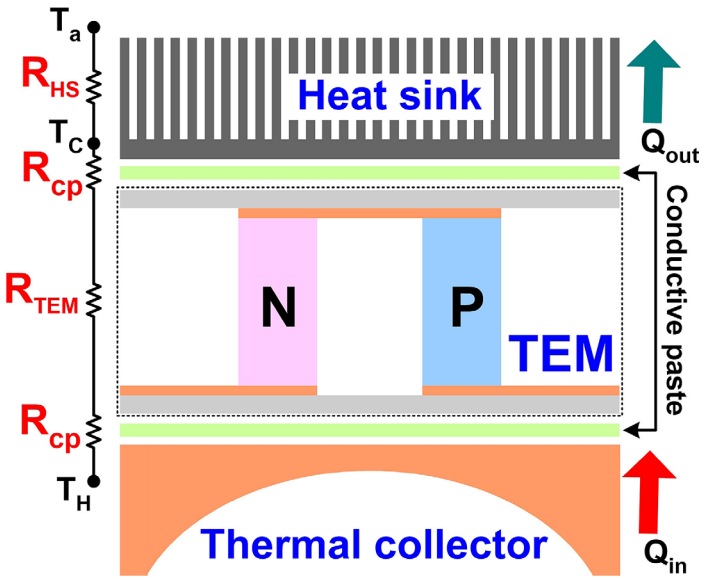

Figure 2. Thermal resistance model of heating block/TEG/heat sink assembly

$$R_{total} = R_{TEM} + 2R_{cp} + R_{HS} \tag{1}$$

We calculated the total heat transfer rate from thermal collectors to ambient air surrounding the heat sink with the following expression [14]:

$$Q_{total} = \frac{T_H - T_a}{R_{total}} \tag{2}$$

with the air temperature T_a and the heating block temperature T_H measured throughout the tests.

The thermal resistance of the heat sink, R_{HS}, was evaluated first, starting from – a dimensional thermal model. This model was based on steady–state heat conduction, which was considered here for the rectangular fin of the heat sink with tip heat loss into the ambient medium.

Assuming that the heat transfer coefficients related to the sink base and the fin, respectively, are constant and equal ($h_b = h_f$), the overall heat rate evacuated by the heat sink Q_{HS} (W) was calculated with the following expression [15]:

$$Q_{HS} = n\theta_b\sqrt{h_f kap}\left[\frac{\tanh(M)+N}{1+N\tanh(M)}\right] + (A-na)\theta_b h_b \tag{3}$$

In relation (3), n represents the number of fins, a (m^2) is the fin base area, A (m^2) is the sink base area, and p (m) is the fin perimeter. M and N are two dimensionless parameters, defined as [15]:

$$M = \left(\frac{h_f p}{ka}\right)^{1/2} \cdot H \text{ and } N = \frac{h_e H}{Mk} \tag{4}$$

Under free convection's influence, we considered h_f = 5 W/m^2·°C and the heat transfer coefficient related to the fin tip h_e = 5 W/m^2·°C [15]. Thermal conductivity for the EN-AW-6060 aluminium alloy material of the heat sink was taken as k = 204 W/m·°C [15]. The temperature difference between the surface of the sink base and the ambient medium, θ_b (°C) is expressed as:

$$\theta_b = T_C - T_a \tag{5}$$

where: T_C is the temperature of the heat sink base, measured during experiments.

The heat sink efficiency, η, represents the ratio between the total heat transfer rate and the heat rate of a sink with ideal thermal behaviour [15]:

$$\eta = \frac{Q_{HS}}{Q_{HS,ideal}} \tag{6}$$

where: the optimum heat transfer rate is [15]:

$$Q_{HS,ideal} = \left[npHh_f + nah_e + (A-na)h_b\right]\theta_b \tag{7}$$

The heat sink effectiveness, ε, is related here to the heat transfer rate developed only through the heat sink base area and is evaluated through relation [15]:

$$\varepsilon = \frac{Q_{HS}}{Ah_b\theta_b} \tag{8}$$

Assuming that there is no heat loss between the base of the heat sink and the ambient air, the overall thermal resistance of the pin-fin heat sink was calculated as [15]:

$$R_{HS} = \frac{1}{A}\left(\frac{1}{\varepsilon h_b} + \frac{t}{k}\right) \tag{9}$$

The calculated heat sink efficiency and effectiveness were $\eta = 0.977$ and $\varepsilon = 14.4$, respectively. With relation (9), we obtained a heat sink resistance $R_{HS} = 5.56$ °C/W.

The thermal resistance of the TEG module, R_{TEM} (°C/W), was evaluated here through the following expression [16]:

$$R_{TEM} = \frac{\Delta T_{\max}}{V_{\max} \cdot I_{\max}} \cdot \frac{2T_h}{\left(T_h - \Delta T_{\max}\right)} \quad (10)$$

In relation (10), $V_{max} = 16$ V and $I_{max} = 6.1$ A, with a maximum temperature of the TEG hot side $T_h = 138$ °C [17]. Assuming a maximum temperature difference between the hot and cold plates of TEG, $\Delta T_{max} = 40$ °C, we obtained $R_{TEM} = 1.83$ °C/W.

The thermal resistance of the interface material R_{cs} (°C/W), silicon-based conductive paste with a low thermal conductivity $k_{cs} = 1.2$ W/m°C, was calculated using the Fourier's law applied along the substrate thickness direction:

$$R_{cs} = \frac{t_{cs}}{A \cdot k_{cs}} \quad (11)$$

We considered a conductive paste thickness $t_{cs} = 0.5$ mm, and $R_{cs} = 0.26$ °C/W. So, the total thermal resistance presented by all the assembly interfaces depicted in Fig. 2 was $R_{total} = 7.91$ °C/W, according to relation (1).

ENERGY AND EXERGY ANALYSIS

Detailed description of the thermoelectric model and system equations used for the present energy analysis are reported elsewhere [18].

The output power of the TEG module was calculated with relation [18]:

$$P_{out} = N\alpha_{TEG} I_L (T_H - T_C) - I_L^2 R_{IN,TEG} \quad (12)$$

where: N = 127 p-n semiconductor couples and α_{TEG} (V/K) is the temperature – dependent Seebeck coefficient for a single TE element, calculated with the correlation [17]:

$$\alpha_{TEG} = 2\times10^{-9} \times \left(22224 + 930.6T_m - 0.9905T_m^2\right) \quad (13)$$

where: $T_m = (T_H + T_C)/2$. We assumed a uniform temperature distribution across the entire heating block surface and considered T_H to be the hot side temperature of the TEG module. The cold side temperature of the thermoelectric device, T_C, was taken as the temperature of the base plate of the heat sink.

In expression 12, the internal resistance of the thermoelectric module $R_{IN,TEG}$ (Ω) was calculated with relation [18]:

$$R_{IN,TEG} = N \times \left(\rho_p \frac{L_p}{A_p} + \rho_n \frac{L_n}{A_n} \right) \quad (14)$$

where: the cross sectional areas and lengths of the p – n semiconductor elements of the Bi_2Te_3 based - TEG module are [18]: $A_p = A_n = 1.96$ mm^2, $L_p = L_n = 1.6$ mm.

The temperature-dependent electrical resistivity of a single Bi_2Te_3 semiconductor leg (Ω/m) was evaluated as [18]:

$$\rho_p = \rho_n = \left(5512 + 163.4T_m + 0.6279T_m^2\right) \times 10^{-10} \quad (15)$$

The energy conversion efficiency of TEG device is calculated wth expression [18]:

$$\eta = \frac{N\alpha_{TEG} I_L (T_H - T_C) - I_L^2 R_{IN,TEG}}{N\left[\alpha_{TEG} T_H I_L + K_{TC}(T_H - T_C)\right] - \frac{1}{2} I_L^2 R_{IN,TEG}} \quad (16)$$

where: the thermal conductance K_{TEG} (W/K) of a sigle thermoelectric element is defined as:

$$K_{TEG} = k_p \frac{A_p}{L_p} + k_n \frac{A_n}{L_n} \quad (17)$$

where: the thermal conductivities k_p and k_n (W/m·K) are considered as [18]:

$$k_p = k_n = \left(62605 - 277.7T_m + 0.4131T_m^2\right) \times 10^{-4} \quad (18)$$

The energy analysis was developed starting from the first law of thermodynamics (conservation of energy) and cannot offer helpful information about the optimal conversion of power [19]. The quality and degradation degree of energy along the thermodynamic process can be evaluated through the concept of exergy [20]. The second law of thermodynamics, associated with the exergy concept, will evaluate here the losses and inefficiencies from the energy conversion process.

The presence of thermodynamic irreversibilities within the energy transfer system is not to be underestimated. These losses, particularly in thermoelectric systems, give rise to exergy destruction issues. We encounter internal irreversibilities such as the Joule heating, heat conduction in thermoelectric legs, and heat losses to the filler material (the structural support). Additionally, there are external irreversibilities including heat transfer at the level of the heat sink, heat source, and fluid source [21].

The central part of the thermoelectric system (without the thermal collector) can be modelled through an exergy flow diagram, presented in Fig. 3. Here, Ex_{HS} is the heat exergy leaving the heat sink and Ex_{power} represents the electrical exergy collected at the TEG output. It was shown that the exergy destruction due to the heat transfer between the cold and hot plates of the TEG modules, $Ex_{dest,TE}$, can be expressed as [21]:

$$Ex_{dest,TE} = \left(1 - \frac{T_a}{T_H}\right) \cdot Q_H - \left(1 - \frac{T_a}{T_C}\right) \cdot Q_C - P_{out} \quad (19)$$

Knowing that the useful electrical power generated by TEG is $P_{TEG} = Q_H - Q_C$ [22], relation (19) became:

$$Ex_{dest,TE} = T_a \cdot \left(\frac{Q_C}{T_C} - \frac{Q_H}{T_H}\right) \quad (20)$$

In relation (20), we identify $S_{gen} = Q_C/T_C - Q_H/T_H$ as the *rate* of entropy generation for TEG module [23].

The reversible work output for the TEG – based energy conversion system will be defined by the relation [24]:

$$W_{rev} = P_{out} + T_a S_{gen} \quad (21)$$

Finally, the exergy efficiency, known also as the second law efficiency, was evaluated trough expression [24]:

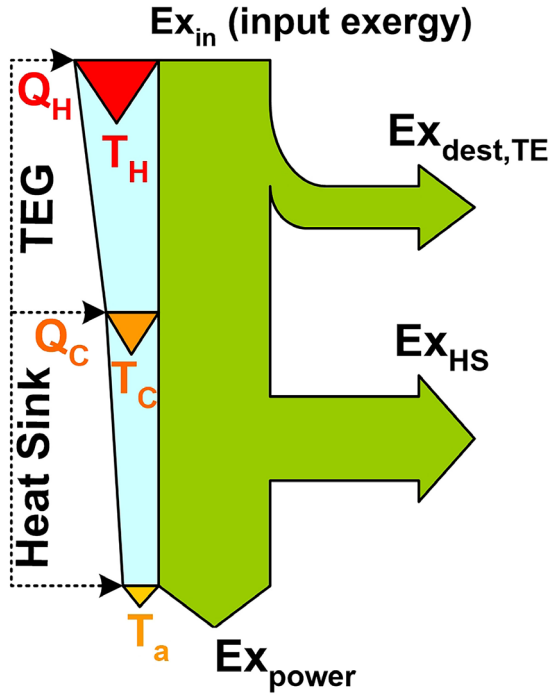

Figure 3. Exergy flow diagram for the TEG/heat sink system

$$\eta_{ex} = \frac{P_{out}}{W_{rev}} = \frac{P_{out}}{P_{out} + T_a S_{gen}} \quad (22)$$

EXPERIMENTAL PROCEDURE

All the experiments were performed on the pipe of the exhaust gas system from a Dacia Logan III 1.0 Tce car, with a gasoline engine having a displacement of 999 cm^3 and a maximum power of 54 kW. The vehicle was tested in static, stationary mode with the engine idle speed between 1000–1500 rpm to simulate the thermal behaviour of an industrial pipeline that generates low-grade heat waste. Figure 4 presents the experimental rig constructed to recover efficiently the waste heat generated by the automotive exhaust pipe.

One side of a copper–made heating block was polished to match the curvature of the pipe. The other side fitted precisely the area of the thermoelectric module, a commercial TEC1 – 12706 device (Hebei I.T. Shanghai, China) with dimensions of 40 × 40 × 3.9 mm^3. The pin fin heat sink is placed in direct contact with the hot side of the TEG module. Three Kafuter K – 523 thin films of thermally conductive paste, having a thermal conductivity of 1.2 W /mK, ensured the heat transfer maximization and optimal adhesion between the pipe, TEG, and heat sink. A simple two–wire clamping method was considered for the entire system assembly.

Temperatures at the external surface of the heating block and the heat sink T_H and T_C were measured using a Perfect Prime TC0304 digital thermometer with K-type thermocouples as temperature sensors. A digital load resistance R_L type SIGLENT SDL 1020X-E DC Electronic Load was connected between TEG module terminals, in parallel with a Peak Tech USB 3315 voltmeter for measuring the output voltage.

RESULTS AND DISCUSSIONS

We performed here two sets of experiments. For the open–circuit voltage test (without load resistance R_L), measurements of U_{OC}, T_H and T_C started to be collected when the temperature difference between the heating block and heat sink $\Delta T = T_H - T_C$ exceeded a value of 20 °C for the first time. This first test was stopped after two minutes, and the measurement results are shown in Fig. 5. We can observe a smooth increase of

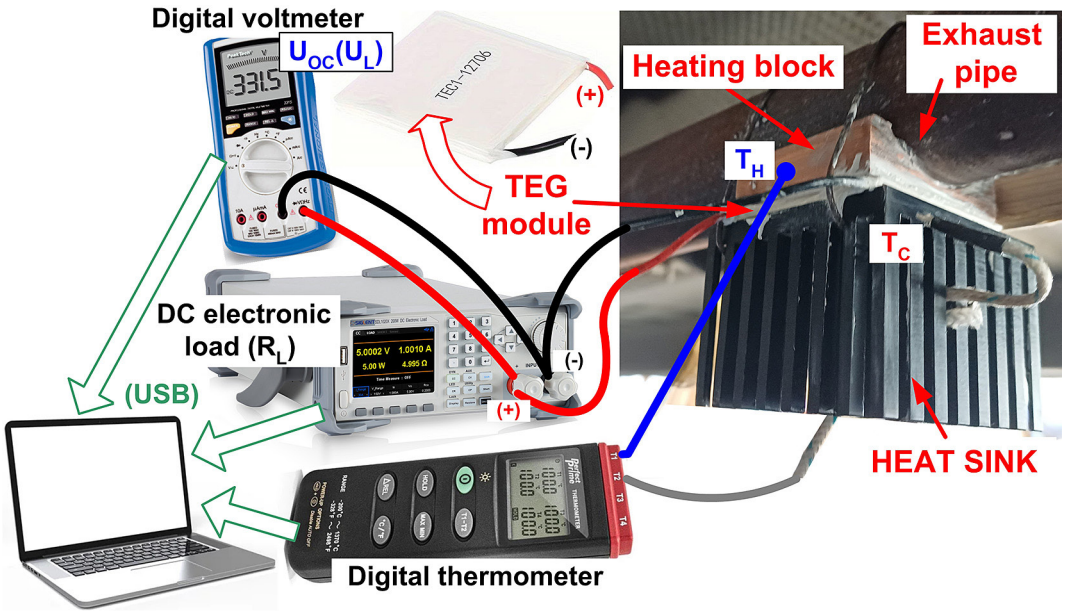

Figure 4. Experimental set – up of the thermoelectric energy conversion system

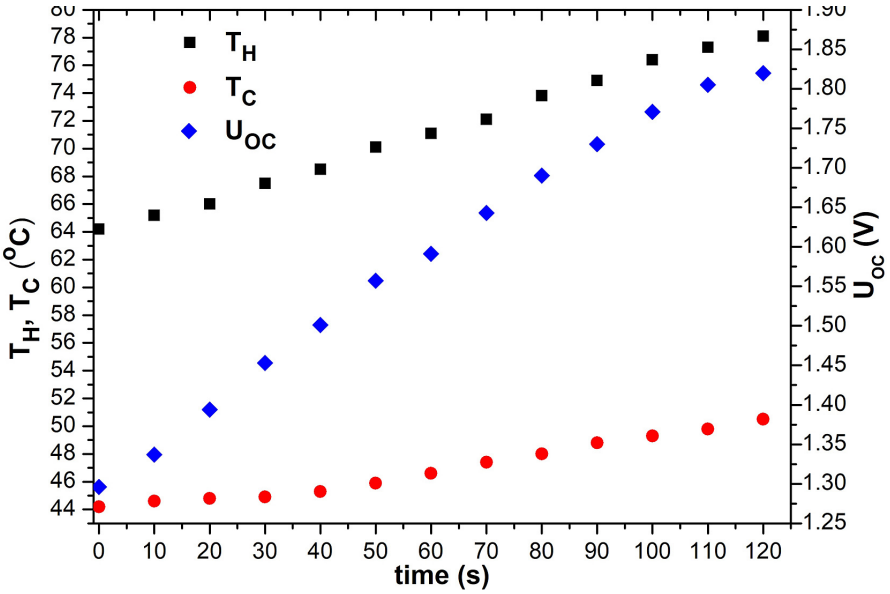

Figure 5. Variations of the heating block and heat sink temperatures, along with open–circuit voltage during the first test.

ΔT, up to 27.6 °C at the end of the test, when U_{OC} reached a maximum value of 1.82 V.

A waste heat harvesting system containing an automotive exhaust pipe, copper thermal collector, single Bi_2Te_3-based TEG module and a liquid cooling system presented an open circuit voltage of 1.8 V at ΔT = 30 °C [25]. From Figure 5, we can see that the same U_{OC} value was attained at ΔT = 27.5 °C, indicating an energy conversion system with similar performances under natural convective cooling of the heat sink (T_C increased with only about 6 °C) at this low-temperature domain of T_H, under 100 °C. Based on the temperature measurements collected during the first experiment, Fig. 6 presents the evolution in time of the thermal energy evacuated by the heat sink and the heat exchanged between the heating block and the ambient air (near the heat sink).

Figure 6 shows that heat transferred from a thermal collector (Q_{total}) was about 15–20% higher than the heat dissipated by the heat sink, Q_{HS}. A 25 % reduction of the parasitic thermal resistance

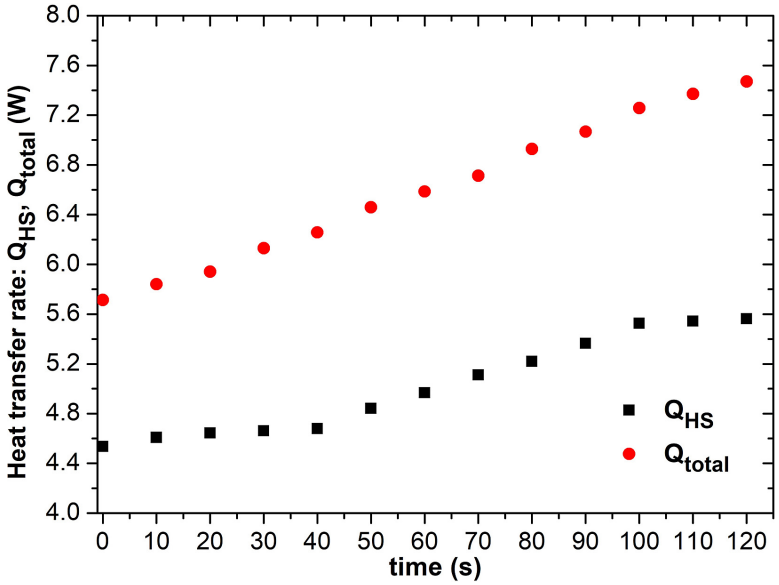

Figure 6. Evolutions of the heat transfer rates between the heat sink and surrounding air and between thermal collector and ambient air T_a = 19 °C.

inside the system will enhance Q_{total} up to 39.5 – 43.5 %. The heat sink resistance R_{HS} represents about 70% of the total thermal resistance, $R_{total.}$ R_{HS} reduction at values under 4 °C/W, offered by another type of passive heat sink, will assure the desired Q_{total} improvement. This way, the quantity of electrical energy converted from the heat waste should increase.

Before the second test (with a duration of eight minutes), we maintained the car with the engine running at idle for about 30 minutes so that the temperature at the level of the heating block would rise as close as possible to 100 °C.

Steady-state behaviour for this type of energy conversion system is fulfilled when the change of U_L is within 1–5 mV for ten consecutive seconds [18]. Consequently, during the second test, R_L was modified gradually from 1 to 80 Ω, with the voltage and temperature data (U_L, T_H and T_C) collected at an interval of 30 s between load resistance stages. Temperatures, voltage and current registered at each R_L value are presented in Fig. 7.

We can see in Fig. 7a that the T_C variation under load resistance change is relatively stable starting from R_L = 10 Ω, benefitting from the efficient cooling of the heat sink with natural air. The same behaviour was also reported in the case of a water–cooling energy conversion system with a commercial Bi_2Te_3 TEG module [26].

Figure 7b indicates through I_L–R_L and U_L–R_L curves a maximum output current and voltage of 0.566 A and 1.658 V, respectively. Variation trend of the output current and voltage curves suggest that the maximum output power of the TEG device should appear at R_L = 3 Ω. It is reported in the literature that the maximum output power of the TEG module was attained when the device's internal resistance R_{IN} matches the load resistance R_L[27]. Also, constant temperature gradient ΔT across TEG should be registered under the optimal ratio R_L/R_{IN} = 1[28].

Figure 8 presents the variations of output power P_{out} and energy conversion efficiency η at different load resistance values. A maximum P_{out} of 0.223 W was attained at R_L/R_{IN} = 1.022. This slight variation from the optimal R_L/R_{IN} is associated with the junction temperature variation at different energy conversion system interfaces under heat load variation. Another Bi_2Te_3 TEG–based energy conversion system with a water-cooled radiator, used for automotive waste heat recovery, generated at T_H = 100 °C, a maximum output power of 0.31 W for a similar R_L value of 3 Ω [29]. A maximum energy conversion efficiency η_{max} of 1.15 % was observed in Fig. 8 when the appropriate combination of voltage and current was 0.925 V and 0.231 A, respectively (see Fig. 7). This maximum value of η was registered at R_L = 4 Ω, slightly higher than R_{IN} (2.95 Ω). Still, this result agrees with other literature reports related to R_L – R_{IN} values for η_{max} [5].

The exergy analysis results are presented in Fig. 9. Here, the exergy efficiency variation and exergy destruction rate (thermodynamic

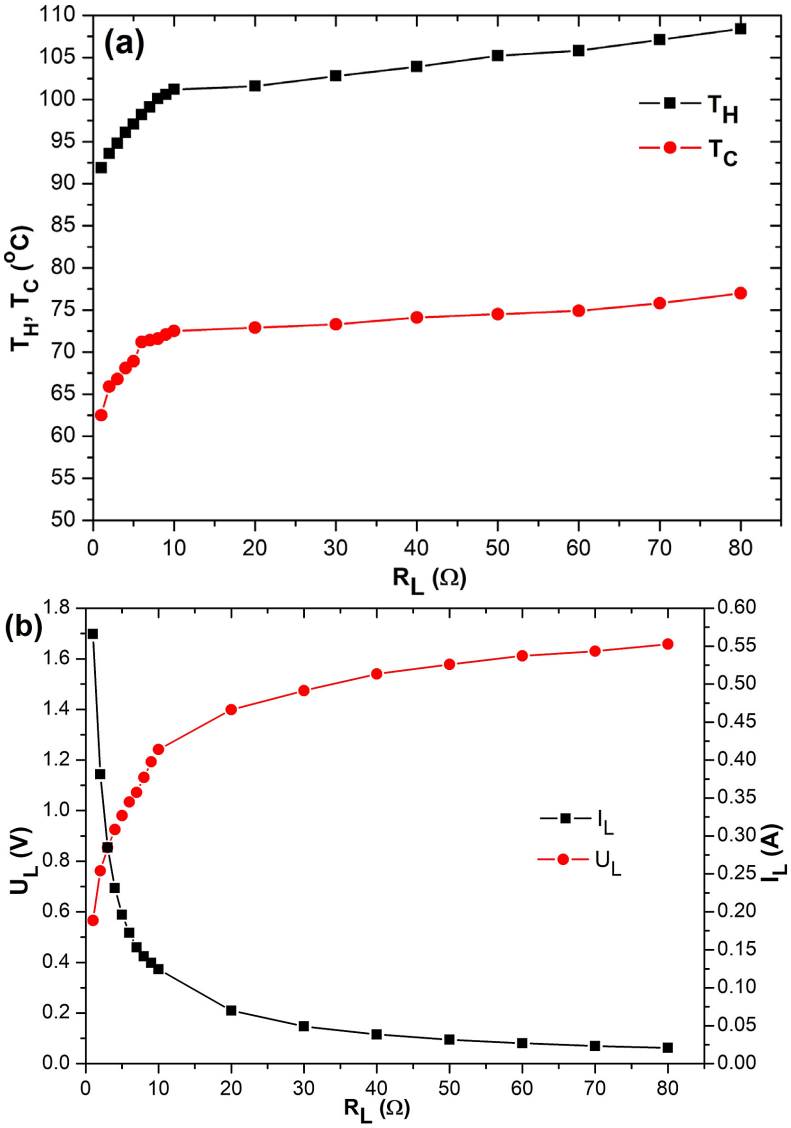

Figure 7. Dependence of (a) heat collector and heat sink base temperatures and (b) output voltage and current on load resistance R_L

irreversibility) inside the TEG module are illustrated as a function of the output system voltage.

From Figure 9 we can see that the exergy efficiency registered a maximum value of 12.42 % at an output voltage of 1.034 V and an output current of 0.172 A, under a low TEG irreversibility value of 1.28 W. We also observed here that, starting from U_L = 1.072 V (R_L = 10 Ω), exergy efficiency presented an abrupt decrease between 11.05 % and 2.91%. Oppositely, the TEG exergy destruction rate remains relatively constant, at values between 1.21 and 1.33 W, due to an almost linear evolution of entropy generation rate S_g at R_L values between 10 and 80 Ω, under a low variation of Q_H and Q_C (less than 1 W). An exciting application of the present energy conversion system can be as a power supply for a sensor–based, indoor air quality monitoring system located in places where other power sources are unavailable nearby. Pollutants like CO, CO_2, and NO_2 can pose a high risk to human health, affecting human decision–making performance in the workplace [30]. An efficient, low – cost and practical energy harvesting system for low–waste heat recovery, used as a power supply for air pollutant sensors, can contain four commercial Bi_2Te_3 TEG modules in a parallel configuration, with natural air-cooled heat sinks and a DC–DC boost converter. This system structure was successful at T_H temperatures between 73 and 90 °C, generating a stable output voltage between 1.8–5 V for output power values over 15 mW [31].

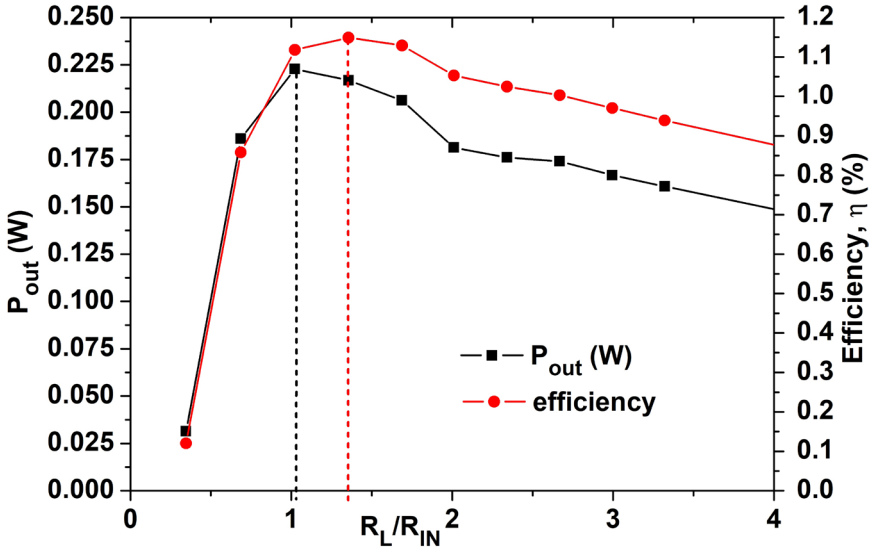

Figure 8. Dependence of output power P_{out} and energy efficiency η on load resistance/TEG internal resistance ratio

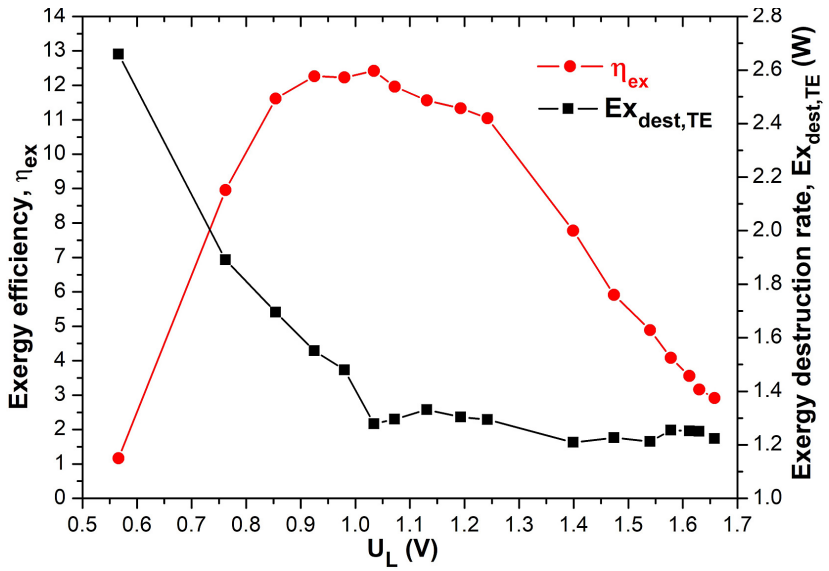

Figure 9. Dependence of the exergy efficiency and TEG internal irreversibility on output voltage U_L

Table 2. The calculated errors for different test instruments

Apparatus	Accuracy	Range	% Error
Thermocouples	±2.2 °C	-40 to 400 °C	0.11
Thermometer	±1 °C	-200 to 200 °C	0.053
Dc electronic load current	1 mA	0 – 30 A	0.048
Dc electronic load voltage	1 mV	0 – 150 V	0.002
Multimeter/voltage	1mV	0 – 4 V	0.002

ERROR ANALYSIS

The errors associated with experimental data were analyzed by considering the accuracy of different instruments used in the study, like thermocouples, digital thermometers, DC electronic loads, and digital multimeters. The instrument's accuracy is presented in Table 2. The

percentage error was calculated with the following relation [32, 33]:

$$Error\% = \frac{Apparatus\ accuracy}{Minimum\ value\ of\ apparatus\ measured} \times 100\% \quad (23)$$

CONCLUSIONS

This paper investigated a TEG–based energy conversion system for waste heat recovery from an engine car's exhaust pipe. A thermal resistance model was applied here for the heating block/TEG/heat sink assembly, and a total thermal resistance (R_{total}) of 7.91 °C/W was estimated for the experimental system. We evaluated the heat transfer rates inside the heat collector and passive heat sink and estimated their percentage contribution to the overall heat transfer improvement across the system. Open–circuit voltage collected between the TEG terminals after two minutes of testing attained a value of 1.8 V under a temperature gradient ΔT = 27.5 °C, similar to the one registered from an energy conversion system with liquid water cooling and the same type of TEG module. A maximum output power of 0.223 W was observed when the load resistance R_L was 3 Ω and the temperature–dependent internal TEG resistance R_{IN} was 2.95 Ω, a similarity which validates the efficient heat transfer development across the system components. Energy conversion efficiency attained a maximum value of 1.15 % at R_L = 4 Ω, when the corresponding current and voltage values were 0.231 A and 0.925 V for ΔT = 28 °C. Instead, exergy efficiency presented a maximum value of 12.42 % at R_L = 6 Ω for U_L/I_L values of 1.034 V/0.172 A at ΔT = 27 °C, with an exergy destruction rate of 1.28 W between the TEG ceramic plates. Future work is planned to implement a similar energy conversion system for heat waste recovery (70 – 100 °C) containing four TEG modules connected in parallel for output power enhancement, cooled by passive heat sinks and coupled with a DC–DC boost converter for an efficient microsensor power supply application.

REFERENCES

1. Bian Q. 2020. Waste heat: the dominating root cause of current global warming, Environ Syst Res 9, 8–19.
2. Xia L., Liu R.M., Zeng Y.T., Zhou P., Liu J.J., Cao X.R., Xiang S.G. 2019. A review of low-temperature heat recovery technologies for industry processes, Chin. J. Chem. Eng. 27, 2227–2237.
3. Xu Z.Y., Wang R.Z., Yang C. 2019. Perspectives for low-temperature waste heat recovery, Energy 176, 1037–1043.
4. Cao Q., Luan W., Wang T. 2018. Performance enhancement of heat pipes assisted thermoelectric generator for automobile exhaust heat recovery. Appl Therm Eng, 130, 1472–9.
5. lbatati F., Attar A. 2021. Analytical and Experimental Study of Thermoelectric Generator (TEG) System for Automotive Exhaust Waste Heat Recovery. Energies, 14(1), 204–2018.
6. Meng J.-H., Gao D.-Y., Liu Y., Zhang K., Lu G. 2022. Heat transfer mechanism and structure design of phase change materials to improve thermoelectric device performance, Energy, 245, 123332.
7. Pfeiffelmann B., Benim A.C., Joos F. 2021. Water-cooled thermoelectric generators for improved net output power: A Review. Energies, 14, 8329.
8. Alsaqoor S. 2023. Performance analysis of a thermoelectric cooler placed between two thermoelectric generators for different heat transfer conditions, Journal of Ecological Engineering, 24(4), 27–35.
9. Li L., Gao X., Zhang G., Xie W.Y., Wang F.F., Yao W. 2019. Combined solar concentration and carbon nanotube absorber for high performance solar thermoelectric generators. Energy Convers. Manag., 183, 109–115.
10. Sateikis I., Ambrulevicius R., Lynikiene S. 2010. Investigations of a micropower thermoelectric generator operating at a low temperature difference. Elektronika Ir Elektrotechnika, 106(10), 113–116.
11. Asaduzzaman Md., Ali Md. H., Nahyan A.P., Nafisa L. 2023. Exhaust heat harvesting of automotive engine using thermoelectric generation technology, Energy Conversion and Management: X, 19, 100398.
12. Mohiuddin A.K.M., Muhammad Y.A., Rahman A., Khan A.A. 2017. Investigation of aluminum heat sink design with thermoelectric generator, IOP Conf. Ser. Mater. Sci. Eng. 184, 012062.
13. Boccardi S., Ciampa F., Meo M. 2019. Design and development of a heatsink for thermoelectric power harvesting in aerospace applications. Smart Mater Struct, 28(10), 105057.
14. Yang Y.T., Peng H.S. and Hsu H.T. 2013. Numerical Optimization of pin-fin heat sink with forced cooling (Int. J. Electron. Commun. Eng.), 7, 884–91.
15. Kon H.S., Lee J.J., Lai C.Y. 2003. Thermal Analysis and Optimal Fin Length of a Heat Sink, Heat Transfer Engineering, 24(2), 18–29.
16. Ajiwiguna T.A., Nugroho R., Ismardi A. 2018. Method for thermoelectric cooler utilization using manufacturer's technical information, AIP Conf. Proc. 1941, 020002. https://asset.re-in.de/add/160267/c1/-/en/000189115DS02/DA_TRU-Components-TEC1-12706-Peltier-Element-15V-

6.4A-65W-L-x-B-x-H-40-x-40-x-3.8mm.pdf, accessed on 20.01.2024.

17. Ionescu V. 2023. Performance analysis of the thermoelectric power – generation system with natural convection cooling, Energy Reports 9, 123–130.
18. Ordonez J.C., Cavalcanti E.J.C. and Carvalho M. 2022. Energy, exergy, entropy generation minimization, and exergoenvironmental analyses of energy systems: A mini-review. Front. Sustain. 3, 902071.
19. da Silva, J.A.M., Ávila Filho, S. and Carvalho, M. 2017. Assessment of energy and exergy efficiencies in steam generators. J. Braz. Soc. Mech. Sci. Eng. 39, 3217–3226.
20. Alsaghir, A.M., Bahk J.H. 2023. Performance optimization and exergy analysis of thermoelectric heat recovery system for gas turbine power plants. Entropy, 25, 1583.
21. Alahmer A., Khalid M.B., Beithou N., Borowski G., Alsaqoor S., Alhendi H. 2022. An experimental investigation into improving the performance of thermoelectric generators, Journal of Ecological Engineering, 23(3), 100–108.
22. Cai Y., Wang W.W., Ding W.T., Yang G.B., Liu D., Zhao F.Y. 2019. Entropy generation minimization of thermoelectric systems applied for electronic cooling: Parametric investigations and operation optimization, Energy Conversion and Management, 186, 401–414.
23. Ali H., Yilbas B.S., Sahin A.Z. 2015. Exergy analysis of a thermoelectric power generator: influence of bi-tapered pin geometry on device characteristics, Int. J. Exergy, 16(1), 53–71.
24. Hsu C.T., Huang G.Y., Chu H.S., Yu B., Yao D.-J. 2011. Experiments and simulations on low-temperature waste heat harvesting system by thermoelectric power generators, Applied Energy, 88, 1291–1297.
25. Cho Y.H., Park J., Chang N., Kim J. 2020. Comparison of cooling methods for a thermoelectric generator with forced convection. Energies, 13, 3185.
26. Kim S. 2013. Analysis and modeling of effective temperature differences and electrical parameters of thermoelectric generators, Applied Energy, 102, 1458–1463.
27. Min G. 2014. Principle of determining thermoelectric properties based on I-V curves. Meas Sci Technol, 25, 85009–85015.
28. Yu C., Chau K.T. 2009. Thermoelectric automotive waste heat energy recovery using maximum power point tracking, Energy Conversion and Management, 50, 1506–1512.
29. Sukor A.S.A., Cheik G.C., Kamarudin L.M., Mao X., Nishizaki H., Zakaria A., Syed Zakaria S.M.M. 2022. Predictive analysis of in-vehicle air quality monitoring system using deep learning technique. Atmosphere, 13, 1587.
30. Mohammadnia A., Rezania A. 2023. Compatibility assessment of TEGs arrangement coupled with DC/DC converter to harvest electricity from low-temperature heat sources, Energy Conversion and Management: X 18, 100356.
31. Mansour M.A., Beithou N., Othman A., Qandil A., Khalid M.B., Borowski G., Alsaqoor S., Alahmer A., Jouhara H. 2023. Effect of liquid saturated porous medium on heat transfer from thermoelectric generator, Int. J. Thermofluids, 17, 100264.
32. Rajaseenivasan T., Srithar K. 2016. Performance investigation on solar still with circular and square fins in basin with CO_2 mitigation and economic analysis, Desalination, 380, 66–74.